FOUR-WAVE INTERACTIONS IN SWAN

Noriaki Hashimoto[1], IJ. G. Haagsma[2], and L. H. Holthuijsen[3]

Abstract: Several methods for computing the non-linear energy transfer due to resonant wave-wave interactions are implemented in an experimental version of the SWAN wave model. These methods and their mutual relationships (illustrating their evolution from one to the other) are described. Of these methods, two are addressed in some detail. Of the first, an approximate method called the modified SRIAM method, the accuracy and efficiency are numerically demonstrated for various directional spectra. The second, an exact method called the FD-RIAM, is up-graded from an earlier version (Hashimoto et al., 1998) on the basis of Komatsu and Masuda (2000) to solve an instability problem caused by singularities in the Boltzmann integral. The accuracy and stability of this exact method too are numerically investigated. This FD-RIAM, supplemented with all other processes of generation and dissipation (and triad wave-wave interactions) in SWAN, is applied to the shallow water Lake George in Australia.

INTRODUCTION

Waves at the surface of the deep ocean can be well predicted with spectral wave models that are driven by predicted wind fields. These models are based on the discrete spectral energy balance equation of individual wave components. In deep water this equation represents the effects of great circle propagation and all processes of generation, dissipation and wave –wave interactions. Amongst these, the non-linear wave-wave interactions dominate the evolution of the wave spectrum. This mechanism causes the energy transfer among an infinite number of component waves. Hasselmann (1962) formulated this mechanism in the form of a Boltzmann integral. The Boltzmann integral, however, includes a complicated coupling coefficient and a singular point,

1 Head, Hydrodynamics Division, Marine Environment and Engineering Department, Port and Airport Research Institute, Independent Administrative Institution, 3-1-1, Nagase, Yokosuka 239-0826 Japan. Hashimoto@pari.go.jp.

2 Research assistant (now Faculty Secretary of Research) , Delft University of Technology, P.O.Box 5048, 2600 GA Delft, The Netherlands, ij. haagsma@ct. tudelft. nl.

3 Associate professor, Faculty of Civil Engineering and Geosciences, Delft University of Technology, P.O.Box 5048, 2600 GA Delft, The Netherlands, l.holthuijsen@ct.tudelft.nl.

which makes the numerical integration difficult, unstable and time-consuming. With the ever increasing computer power, new attempts can be made to introduce this mechanism into a wave model as accurately and as efficiently as possible.

The third-generation wave model WAM that is used in many countries, adopts the Discrete Interaction Approximation (DIA; Hasselmann and Hasselmann, 1985), to compute the quadruplet wave-wave interactions. Introducing the DIA into third-generation wave modelling has greatly improved the response of wave models to complex variations of wind field compared with previous (first- and second-generation) wave models. However, the DIA has a drawback in that it gives a poor approximating of the interactions in the case of narrow spectra such as the JONSWAP spectrum although it gives good results for broad spectra such as the Pierson-Moskowitz spectrum.

A shallow-water version of WAM has been developed for the simulation and prediction of waves in a variety of near-shore, shallow water conditions with ambient currents (Booij et al., 1999). This model, SWAN (Simulating WAve Nearshore) accounts for wave generation by wind, shoaling, refraction due to current and depth, frequency shifting due to currents and non-stationary depth, three- and four-wave interactions, whitecapping, bottom friction, depth-induced breaking; wave-induced set-up, transmission through and reflection from obstacles, etc. The deep-water formulations are taken from WAM, including the DIA. In shallow water the quadruplet interactions are approximated by multiplying the deep-water interactions with a depth dependent scaling (in SWAN as in WAM) which is rather a crude approximation.

In the present paper, we introduce several methods that have been implemented into SWAN for computing the quadruplet wave-wave interactions
for deep water:

- one exact method (the RIAM method; Masuda,1980; Komatus and Masuda, 1997) and
- two approximate methods (the multiple DIA and the modified SRIAM method; Komatsu and Masuda, 1996, Hashimoto and Kawaguchi, 2001) and

for finite-depth water:

- one exact method (an up-graded FD-RIAM; Hashimoto, et al., 1998; Komatsu and Masuda, 2000).

Although some of the methods have been published and others not, we will briefly explain all these methods. We will examine their accuracy and efficiency through numerical computations and we will give an example of a real 2D-case with observations in finite-depth water.

QUADRUPLET WAVE-WAVE INTERACTIONS

Probably the best known derivation of the four-wave interactions is due to Hasselmann (1962) who showed that three wave components of the wave action density spectrum of random, short-crested waves can interact with a fourth component. The equation is known as the Boltzmann integral and is expressed by the following equation:

$$\frac{\partial n(\mathbf{k}_4)}{\partial t} = \int\cdots\int d\mathbf{k}_1 d\mathbf{k}_2 d\mathbf{k}_3 G(\mathbf{k}_1,\mathbf{k}_2,\mathbf{k}_3,\mathbf{k}_4)\delta(\mathbf{k}_1+\mathbf{k}_2-\mathbf{k}_3-\mathbf{k}_4) \times \delta(\omega_1+\omega_2-\omega_3-\omega_4)\{n_1 n_2(n_3+n_4)-n_3 n_4(n_1+n_2)\} \quad (1)$$

where, $n(\mathbf{k}_i)$ is the action density, $\mathbf{k}$ is the wave number vector, ω is the angular frequency, satisfying the dispersion relationship: $\omega_i^2 = gk_i \tanh k_i h$, and G is the coupling coefficient. The delta functions in the integration represent the resonant conditions among four wave components

$$\mathbf{k}_1+\mathbf{k}_2=\mathbf{k}_a=\mathbf{k}_3+\mathbf{k}_4 \quad \text{and} \quad \omega_1+\omega_2=\omega_a=\omega_3+\omega_4. \quad (2)$$

This implies transfer of action across the spectrum such that the spectrum evolves to lower and lower frequencies and that under active wind conditions, its shape tends to evolve towards a JONSWAP spectrum (Hasselmann et al., 1973).

The expression that represents the four-wave interactions is rather complicated. It involves a six-fold integral in spectral space with resonant conditions where the wave components interact. These resonant conditions (based on the linear dispersion relationship of ocean surface waves) allow the reduction of the six-fold integral to a three-fold integral. The result of this reduction depends on which choice is made as to which of the independent variables are eliminated. In the past, several attempts have been made for deep- and finite-depth conditions, resulting in different approaches in the numerical codes (e.g., the EXACT-NL code of Hasselmann and Hasselmann, 1981; or the WRT code of Webb, 1978 and Tracy and Resio, 1982). The DIA technique in WAM and SWAN is essentially a reduction of the approach of the EXACT-NL code from a very large number of sets of four waves (quadruplets) to only one such quadruplet and its mirror image (in **k**-space). In finite-depth water the same approach as in deep water could be taken but to the best of our knowledge that has not been done yet.

In the present study, we describe an exact method for deep water (the RIAM code; Masuda, 1980: Komatsu and Masuda, 1996) and an exact method for finite-depth water (the FD-RIAM; Hashimoto et al., 1998; Komatsu and Masuda, 2000). The RIAM method is reduced to an approximate method (the SRIAM) in a way similar to the DIA which has been expanded to obtain higher accuracy in deep water (Komatsu, 1996).

The basic difference with the RIAM on the one hand and EXACT-NL and the WRT codes on the other is that the frequency and directions $(\theta_1, \omega_3, \theta_3)$ are taken as independent variables where EXACT-NL and the WRT codes take other independent variables.

DEEP WATER

The RIAM method (exact method)

The methods described in this paper were all developed from the initial work of Masuda (1980). Masuda (1980) derived a reduction of the six-fold Boltzmann integral

to a three-fold integral by taking the independent parameters $(\theta_1, \omega_3, \theta_3)$ as expressed by the following equation;

$$\frac{\partial \phi_4}{\partial t} = (2\omega_4^{23}) \int_0^{\pi} d\tilde{\theta}_3 \int_0^{\infty} d\tilde{\Omega} \int_0^{\pi} d\tilde{\theta}_1 \sum_{\pm} \sum_{\pm} \sum_{\pm} (8\tilde{\omega}_1^3 \tilde{\omega}_3^4 \tilde{G} S^{-1}) \{n_1 n_2 (n_3 + n_4) - n_3 n_4 (n_1 + n_2)\} \quad (3)$$

where, $|\mathbf{k}_1| \leq |\mathbf{k}_2|$ (or $\omega_1 \leq \omega_2$) is assumed without loss of generality from the symmetry of Eq. (1). The variables are non-dimensionalised by

$\tilde{\theta}_1 = \theta_1 - \theta_a$, $\tilde{\theta}_2 = \theta_2 - \theta_a$, $\tilde{\theta}_3 = \theta_3 - \theta_4$, $\tilde{\omega}_1 = \omega_1 / \omega_4$, $\tilde{\omega}_2 = \omega_2 / \omega_4$, $\tilde{\omega}_3 = \omega_3 / \omega_4$, and $\tilde{\Omega} = \ln \tilde{\omega}_3$.

The denominator *S* arising from $\delta(\omega_1 + \omega_2 - \omega_3 - \omega_4)$ is given by

$$S = \left| 1 + (\omega_1/\omega_2)\{(\omega_1/\omega_2)^2 - (|\mathbf{k}_a|/\omega_2^2)\cos(\theta_1 - \theta_a)\} \right| \quad (4)$$

Fig. 1 shows schematically the domain of integration in the $(\tilde{\theta}_1, \tilde{\Omega}, \tilde{\theta}_3)$ space. It is an infinitely long rectangular prism exclusive of a lower region resulting from the condition $\omega_1 \leq \omega_2$. This excluded volume is bounded by three planes $\tilde{\theta}_3 = \pi$, $\tilde{\Omega} = 0$, $\tilde{\theta}_1 = 0$, and a curved surface $\tilde{\theta}_1 = \theta(\tilde{\theta}_3, \tilde{\Omega})$. The singular points caused by the denominator S^{-1} are located along a curve $\gamma = |\mathbf{k}_a|^{1/2} \omega_a^{-1} - 2^{-1/2} = 0$ on the plane $\tilde{\theta}_1 = 0$.

As Masuda noted, a numerical instability in the integration of Eq. (3) is caused mainly by inappropriate treatment of singular points. Masuda hence solved this instability problem by analytically deriving an approximate solution of Eq. (3) around the singular points.

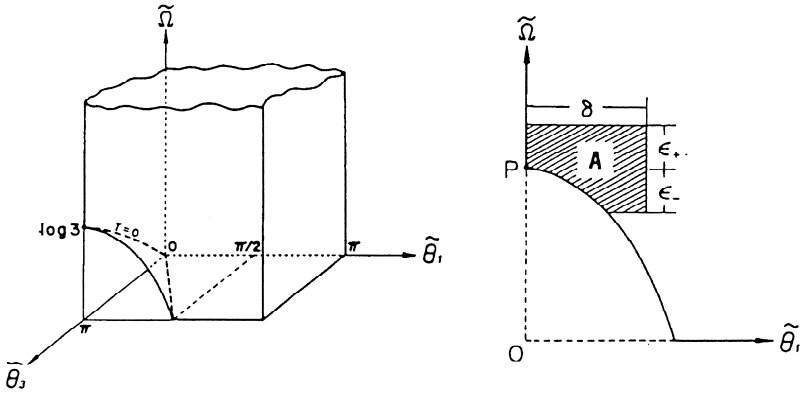

Fig. 1 A schematic graph of the region over which the integration (Eq. 3) is performed (left figure) and a schematic graph of a cross section ($\tilde{\theta}_3$=constant) of the left rectangular prism, at which the singular point P exists (right figure) (Masuda, 1980).

In order to improve the performance of wave models with the above technique of Masuda and to gain better physical understanding of the spectral evolution, Komatsu and Masuda (1996) developed a new scheme called the RIAM method (RIAM = Research Institute for Applied Mechanics, Kyushu University, Japan) for calculating the non-linear energy transfer on the basis of the rigorous method of Masuda (1980). This new scheme was developed by taking advantage of the symmetry of the integrand as in Hasselmann and Hasselmann (1981) or Resio and Perrie (1991), and by truncating less significant configurations of resonance to achieve shorter computational time without loss of accuracy.

As Komatsu and Masuda (1996) mentioned, there are two kinds of symmetries in the resonant interaction. The first is based on the well-known nature of non-linear resonant interactions among gravity waves expressed by Eq. (1). As explained in Hasselmann and Hasselmann (1981), $\delta n(\mathbf{k}_i)d\mathbf{k}_i/\delta t$ (i =1, 2, 3, 4) have the following relationship:

$$\frac{\delta n(\mathbf{k}_1)}{\delta t}d\mathbf{k}_1 = \frac{\delta n(\mathbf{k}_2)}{\delta t}d\mathbf{k}_2 = -\frac{\delta n(\mathbf{k}_3)}{\delta t}d\mathbf{k}_3 = -\frac{\delta n(\mathbf{k}_4)}{\delta t}d\mathbf{k}_4 \tag{5}$$

where $\delta n(\mathbf{k})/\delta t$ indicates the action transfer that is due to this particular resonance combination. As shown in Equation (5), $\delta n(\mathbf{k}_i)d\mathbf{k}_i/\delta t$ (i =1, 2, 3, 4) are of equal magnitude but are different in sign. Accordingly, if we calculate $\delta n(\mathbf{k})/\delta t$ for one component of the resonant four waves, then we immediately know $\delta n(\mathbf{k})/\delta t$ for the other three components. The other type of symmetry is associated with the geometrical similarity of resonance configurations. One is the mirror image of a resonance combination that has the same interaction coefficient as the original one. The other is a rotation of a resonance combination that also gives the same interaction coefficient.

Now, we specify a particular wave number vector $\mathbf{k}_4$ (with ω_4 and θ_4) at which the non-linear energy transfer is to be evaluated, and then assume the sequence of frequencies as follows, considering the first kind of symmetry of the non-linear wave-wave interaction so as to eliminate the overlap computations.

$$\omega_3 \le \omega_1 \le \omega_2 \le \omega_4 \tag{6}$$

For the computation of realistic continuous energy transfer of $\partial n(\omega,\theta)/\partial t$, the computation must be carried out with the loops of frequency ω_4 and direction θ_4. The computation of the configuration of resonant interactions are to be performed in advance with the computation of variables such as $\tilde{G}$, S, $\cdots\cdots$ in the Boltzmann integral for both regular and singular points. The details of the computation procedure are explained in Masuda (1980) and Komatsu and Masuda (1996).

The SRIAM method (approximate method)

The RIAM method turned out to have the same degree of accuracy as Masuda's rigorous method. Although the RIAM method is 300 times faster than Masuda's method, it is still a few thousands times slower than the DIA, simply because the RIAM method processes thousands of resonance configurations.

Hence, Komatsu (1996) developed a new scheme of practical efficiency with a slightly lower level of accuracy than the RIAM method. The method is called the Simplified RIAM (SRIAM) method, which processes 20 representative configurations chosen by some optimisation. The SRIAM method can be expressed by the following equation.

$$T(\omega_4,\theta_4)=\frac{\partial \phi_4}{\partial t}=(2\omega_4^{23})\sum_{i=1}^{20} C_i \tilde{K}_i(\tilde{\theta}_1,\tilde{\Omega},\tilde{\theta}_3)\{n_1 n_2 (n_3+n_4)-n_3 n_4 (n_1+n_2)\}_i \qquad (7)$$

where $\tilde{K}_i(\tilde{\theta}_1,\tilde{\Omega},\tilde{\theta}_3)=8\tilde{\omega}_1^3\omega_3^4\tilde{G}S^{-1}\Delta\tilde{\theta}_3\Delta\tilde{\Omega}\Delta\tilde{\theta}_1$, and C_i, $(i=1,\cdots 20)$ are the coefficients.

Komatsu (1996) listed the optimum 20 combinations of the resonant configurations as well as the optimum positive coefficients C_i tuned by some optimisation, where 7 configurations are chosen for singular points and the other 13 configurations are chosen for regular points from $(\tilde{\theta}_1,\tilde{\Omega},\tilde{\theta}_3)$ space (**Fig. 1**).

It is noted that in the method of Komatsu (1996) the optimum resonant configurations and the coefficients C_i depend on how many configurations we choose as well as how many directional and frequency bins constitute the directional spectrum in the model. That is, the optimum resonant configurations and the coefficients C_i have to be re-determined for each different computation conditions. For these reasons, a simpler method is preferable to determine the optimum configurations and the coefficients C_i.

We therefore simply applied a least square method for Eq. (7) with the exact values of $T(\omega_4,\theta_4)$ (obtained with RIAM) so as to estimate the optimum coefficients C_i, and examined the accuracy and efficiency of the method. We call this simplified method the modified SRIAM method to distinguish it from the original SRIAM method.

Fig. 2 is an example of the computations of the non-linear energy transfer for various directional spectra. The upper panels in the figure show the exact values computed by the RIAM method, the middle panels show approximate values computed by the modified SRIAM method. These panels express the non-linear energy transfer as a function of frequency and direction, where the solid and the dotted lines show negative and positive values, respectively. The values of the upper and middle panels were integrated with respect to the direction and shown as the function of frequency in the lower panels. The values in these figures were normalized by the maximum absolute value of the exact value of the non-linear energy transfer. As shown in **Fig. 2**, the modified SRIAM shows good agreement with the exact values of the RIAM regardless of the shape of the directional spectra.

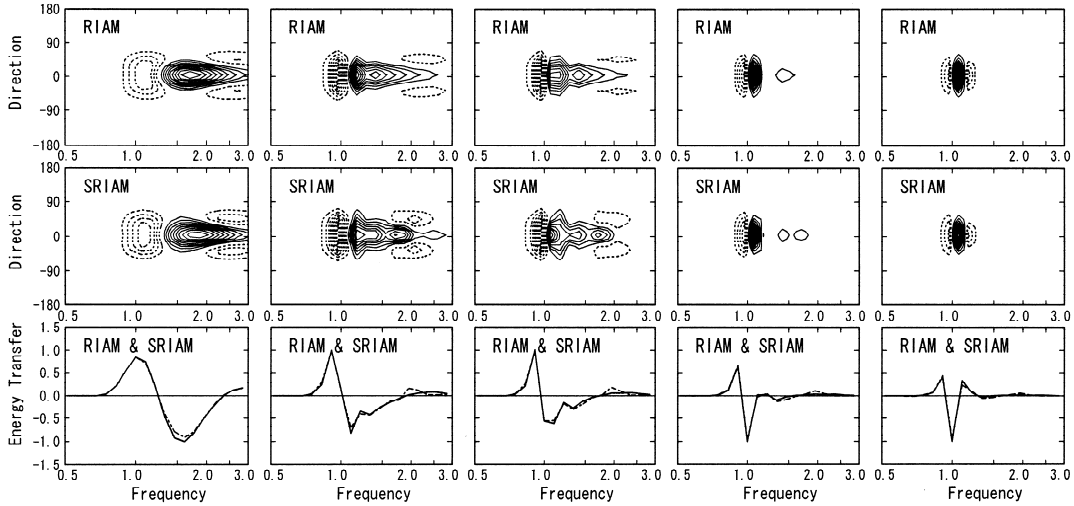

Fig. 2 Comparison of the deep-water quadruplet interactions computed by the exact RIAM method and the approximate modified SRIAM method for various directional spectra.

The MULTIPLE-DIA method (approximate method)

Whereas the original DIA simplifies the computation by adopting one single configuration of the resonant four wave components, the SRIAM method adopts 20 configurations by selecting effective configurations that contribute significantly to the Boltzmann integral. The SRIAM method has demonstrated that it makes the computation 100 times faster than RIAM while retaining most of RIAM's accuracy in computing the non-linear energy transfer. The SRIAM is thus almost perfect with respect to accuracy and versatility to compute the non-linear energy transfer for deep-water waves. However, it requires a computation time 20 times longer than the DIA which is still considered to be impractical for operational wave models.

On the other hand, Hashimoto and Kawaguchi (2001) examined the validity and the effectiveness of the original DIA on the basis of the accuracy of the computations for several directional spectra. They also demonstrated that the accuracy of the approximation generally improves as the number of the configurations in the DIA increases and that such a version with only a few configurations (the extended DIA) can well approximate the non-linear energy transfer for a normal directional spectrum having a single energy peak. Introducing more coefficients and thus more freedom in the EDIA resulted in the multiple DIA (MDIA; Ueno and Ishizaka, 1997).

The EDIA and the MDIA are expressed by the following equations, respectively:

$$\begin{Bmatrix} \delta S_{nl} \\ \delta S_{nl}^{+} \\ \delta S_{nl}^{-} \end{Bmatrix} = \sum_i \begin{Bmatrix} -2(\Delta\omega\Delta\theta)/(\Delta\omega\Delta\theta) \\ (1+\lambda_i)(\Delta\omega\Delta\theta)/(\Delta\omega_{+}\Delta\theta) \\ (1-\lambda_i)(\Delta\omega\Delta\theta)/(\Delta\omega_{-}\Delta\theta) \end{Bmatrix} C_i \omega^{11} g^{-4} \left[F^2 \left\{ \frac{F_{+}}{(1+\lambda_i)^4} + \frac{F_{-}}{(1-\lambda_i)^4} \right\} - 2\frac{FF_{+}F_{-}}{(1-\lambda_i^2)^4} \right] \tag{8}$$

$$\begin{Bmatrix} \delta S_{nl} \\ \delta S_{nl}^{+} \\ \delta S_{nl}^{-} \end{Bmatrix} = \sum_i \begin{Bmatrix} -2(\Delta\omega\Delta\theta)/(\Delta\omega\Delta\theta) \\ (1+\lambda_i)(\Delta\omega\Delta\theta)/(\Delta\omega_{+}\Delta\theta) \\ (1-\lambda_i)(\Delta\omega\Delta\theta)/(\Delta\omega_{-}\Delta\theta) \end{Bmatrix} \omega^{11} g^{-4} \left[C_{1,i} F^2 \left\{ \frac{F_{+}}{(1+\lambda_i)^4} + \frac{F_{-}}{(1-\lambda_i)^4} \right\} - 2C_{2,i} \frac{F F_{+} F_{-}}{(1-\lambda_i^2)^4} \right] \tag{9}$$

where F is the spectrum, $F \equiv F(\omega,\theta)$, $F_{+} \equiv F(\omega_{+},\theta)$, $F_{-} \equiv F(\omega_{-},\theta)$, and λ is the parameter controlling the interaction configurations.

Hasselmann and Hasselmann (1985) adopted the value of $\lambda = 0.25$ in the original DIA. When λ is specified, the four wave configurations are determined by the following equations,

$$\left.\begin{aligned} &\omega_1 = \omega_2 = \omega \\ &\omega_3 = \omega(1+\lambda) = \omega_{+} \\ &\omega_4 = \omega(1-\lambda) = \omega_{-} \\ &\theta_1 = \theta_2 = \theta \end{aligned}\right\} \text{ and } \left.\begin{aligned} &\theta_3 - \theta = \pm\cos^{-1}\left\{\frac{1+2\lambda+2\lambda^3}{(1+\lambda)^2}\right\} \\ &\theta_4 - \theta = \mp\cos^{-1}\left\{\frac{1-2\lambda-2\lambda^3}{(1+\lambda)^2}\right\} \end{aligned}\right\} \tag{10}$$

As seen in these equations, the EDIA was developed by increasing the number of configurations, each of which has different parameters λ_i and C_i. The MDIA was developed by introducing additional parameters $C_{i,1}$ and $C_{i,2}$ into the EDIA. The optimum parameters C_i, $C_{i,1}$ and $C_{i,2}$ included in the EDIA and the MDIA were determined by minimizing the errors between the exact values (RIAM) and their approximate values for several directional spectra. The efficiency and accuracy of the EDIA and the MDIA were examined for several directional spectra and computational conditions. The resulting optimum parameters λ_i and C_i for the EDIA and λ_i, $C_{i,1}$ and $C_{i,2}$ for the MDIA are listed in Hashimoto and Kawaguchi (2001).

FINITE-DEPTH WATER

The FD-RIAM method (exact method)

Although the RIAM method, the SRIAM method, and the multiple DIA method, compute the non-linear energy transfer accurately compared with the DIA, they only apply to deep-water waves. The non-linear quadruplet interactions for finite depth in WAM and the public -domain SWAN are approximated by multiplying the deep-water transfer rate (computed with the DIA) with a depth dependent scaling factor *R*. Although this approximation provides a convenient, first-order representation of the change in magnitude of the non-linear energy transfer, this does not capture the frequency shift and the spectral shape changes that occur as water depth decreases.

Hashimoto et al. (1998) proposed a computational method for calculating the non-linear energy transfer in finite-depth gravity wave spectra, by extending the exact methods for deep water of Masuda (1980) and Komatsu and Masuda (1996; i.e., the RIAM method). It involves reducing the Boltzmann integral for finite-water depth as follows,

$$\frac{\partial\phi(\omega_4,\theta_4)}{\partial t}=\frac{2\omega_4 k_4}{C_g(k_4)}\int d\tilde{\theta}_3\int d\Omega\int d\tilde{\theta}_1\left\{\frac{k_1k_3\omega_3}{C_g(k_1)C_g(k_3)}\frac{G}{S}\right\}\{n_1n_2(n_3+n_4)-n_3n_4(n_1+n_2)\} \quad (11)$$

where $\tilde{\theta}_1=\theta_1-\theta_a$, $\tilde{\theta}_2=\theta_2-\theta_a$, $\tilde{\theta}_3=\theta_3-\theta_4$, $\Omega=\ln\omega_3$ and the denominator *S*, arising from $\delta(\omega_1+\omega_2-\omega_3-\omega_4)$, is given by

$$S=\left|1+\frac{C_g(k_2)}{C_g(k_1)}\left\{\frac{k_1-k_a\cos(\theta_1-\theta_a)}{k_2}\right\}\right| \quad (12)$$

Comparing the difference between the deep- and finite-depth results of Hashimoto's method and those of EXACT-NL (Hasselmann and Hasselmann, 1981), Hashimoto's method seems to have an equivalent or better accuracy than those of EXACT-NL since EXACT-NL's results include unstable "zigzag" shapes even for the case of deep-water waves. Hashimoto's results, however, still include some instability for the case of finite-depth waves even though he used an analytical solution around the singular points of the Boltzmann integral, in the same way as Masuda (1980) for deep-water waves.

Recently, Komatsu and Masuda (2000) pointed out that these instabilities originate in the nature of the four wave resonance interactions in finite-water depth. That is, the shape of the resonance interaction contour lines becomes flatter in finite-water depth compared with that of deep-water depth as shown in **Fig. 3**. Accordingly, a small change of $\tilde{\theta}_1$ on the resonance interaction contour lines of finite-water depth causes great differences in the magnitude of ω_1 as well as the integrand of the Boltzmann integral compared with those of deep-water depth, and this results in unstable computations. Therefore, in order to eliminate the instability of the computations, Komatsu and Masuda (2000) changed the sequence of frequencies of Eq. (6) in integrating Eq. (11) as follows,

$$\omega_1\le\omega_3\le\omega_4\le\omega_2 \quad (13)$$

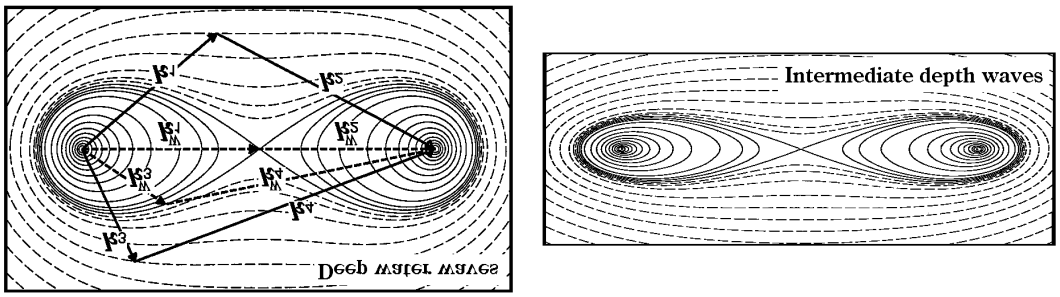

Fig. 3 Resonance interaction charts for deep-water waves (left figure) and intermediate-water waves (right figure).

It is noted that by introducing this modification, the special treatment of the integration around the singular points is no longer necessary. That is, in the RIAM computations, the integration area of the Boltzmann integral with respect to $\tilde{\theta}_1$ and $\tilde{\theta}_3$ was reduced to the area B in **Fig. 4** by assuming the order of Eq. (6), which was originally assumed to eliminate the overlap computations and successfully reduced the computation time. Unfortunately, in this case, the singular point exists in the area B, and a careful treatment is necessary to integrate around the singular point.

On the other hand, by assuming the order of Eq. (13) instead of Eq. (6), the integration area with respect to $\tilde{\theta}_1$ and $\tilde{\theta}_3$ becomes the area A instead of the area B in **Fig. 4**. Although the area A is larger than area B and requires a longer computation time for the integration, there is fortunately no singular point in the area A, which makes the integration stable and accurate. Note that the difference of the rectangular prism in **Fig. 1** and **Fig. 4** is due to the difference of sequence of ω_3 and ω_4. In Masuda (1980), $\omega_3 \geq \omega_4$ is assumed in **Fig. 1**.

In addition, in the RIAM method for deep-water waves, the values on the resonant wavenumber vectors are simply replaced with the values on the nearest wavenumber grid points without loss of accuracy (Komatsu and Masuda, 1996). However, this does not apply to finite-depth water computations where interpolated values of the surrounding four wave numbers are needed (Komatsu and Masuda, 2000). The method thus developed is called the Finite-Depth RIAM (FD-RIAM). It is obviously also applicable for deep water as a special case of finite-depth water.

Fig. 5 shows the examples of the computations of the FD-RIAM for deep- and finite-water wave spectra. As shown in **Fig. 5**, the intensity of the non-linear energy transfer increases and the positive peak frequency moves toward lower frequency side as the relative water depth $k_p h$ decreases (this cannot be achieved with the depth scaling of the DIA).

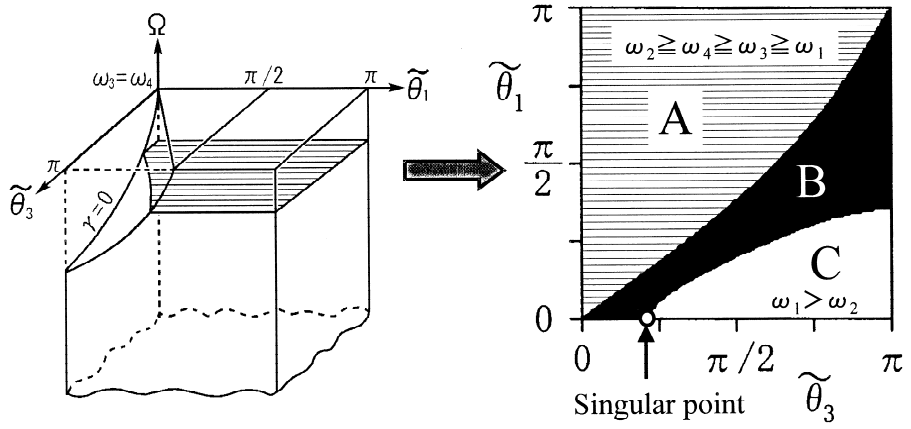

Fig. 4 A schematic graph of a cross section (Ω=constant) of the rectangular prism in **Fig. 1**.

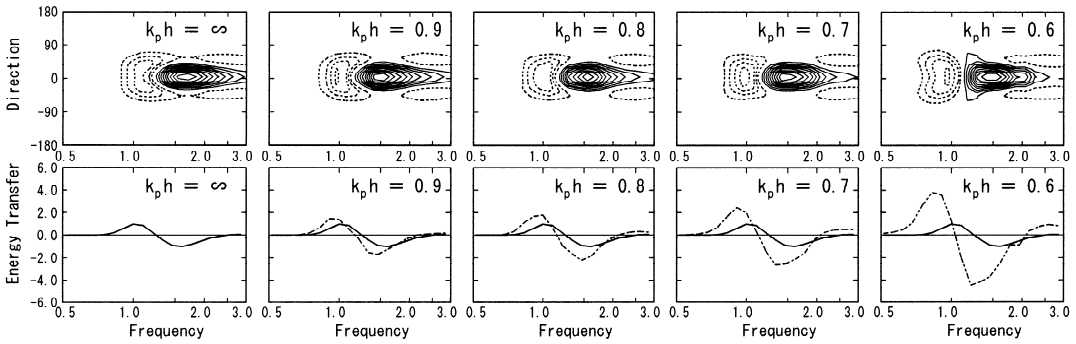

Fig. 5 Examples of the computations of the non-linear energy transfer for finite-water wave spectra. (The solid lines in the lower panels show the non-linear energy transfer for deep-water wave spectrum. The dashed lines show those of finite-water wave spectra. The values in these figures were normalized by the maximum absolute value of the non-linear energy transfer for deep-water wave spectrum.)

The implementation of the FD-RIAM code in SWAN allows us to compute real 2-D field cases with highly accurate computations of the four-wave interactions, supplemented with all other processes of generation and whitecapping (and triad wave-wave interactions). This is probably the first time that this has been done. It may be emphasized that for shallow water the code computes the interactions without depth-scaling deep water computations. One of the cases that we have considered is a near-ideal 2-D case of wave generation in the shallow water Lake George in Australia (Young and Verhagen, 1998). **Fig. 6** gives wave spectra in Lake George as observed by Young and Verhagen (1996) and as computed by SWAN with the DIA and the FD-RIAM. The results with the FD-RIAM obviously improve the computed shape of the spectrum as shown in **Fig. 6**. During the growth phase of the waves the improvement in the calculations due to the FD-RIAM method is most notable at the low frequency end of the spectrum In this finite depth case the low frequency part of the (positive) non-linear energy transfer is much larger than when a uniform depth-scaling is applied. Further research is necessary to draw more general conclusions with respect to this effect. However, the FD-RIAM method is still very expensive in terms of computer effort and we will therefore have to develop a new method with a reduced approach in the very near future.

CONCLUSIONS

We implemented several methods for computing the quadruplet wave-wave interactions: for deep water the exact method of RIAM and the approximate methods of the multiple DIA and the (modified) SRIAM and for finite-depth water the exact method of FD-RIAM. These methods can provide accurate and reliable values of the non-linear energy transfer, which are useful not only for operational purposes but also for scientific purposes to gain better understanding of the physics of spectral evolution.

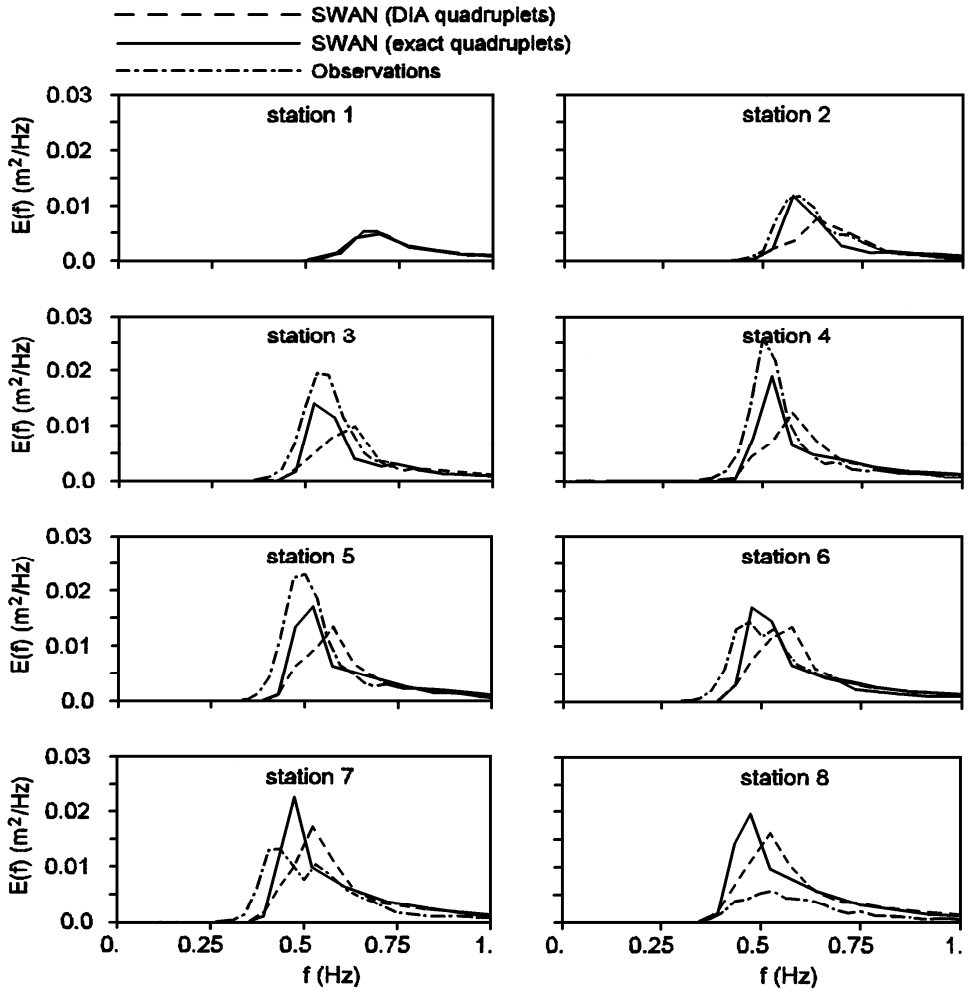

Fig. 6 The wave spectra in Lake George as observed by Young and Verhagen (1996; dash-dot lines) and as computed by SWAN with the DIA approximation (dashed lines) and the exact FD-RIAM (solid lines) for finite-water depth.

REFERENCES

Booij, N., R. Ris and L.H. Holthuijsen, 1999, A third-generation wave model for coastal regions, Part I, Model description and validation, *Journal of Geophysical Research*, Vol. 104, No.C4, 7649-7666.

Hashimoto N., H. Tsuruya and Y. Nakagawa, 1998, Numerical computations of the nonlinear energy transfer of gravity-wave spectra in finite water depths, *Coastal Engineering Journal*, 40, World Scientific, 23-40.

Hashimoto, N and K. Kawaguchi, 2001, Extension and Modification of Discrete Interaction Approximation (DIA) for Computing Nonlinear Energy Transfer of Gravity Wave Spectra, *Proc. 4th Int. Symp. Waves 2001*, 530-539.

Hasselmann, K., 1962, On the non-linear energy transfer in a gravity-wave spectrum, Part 1, General theory, *Journal of Fluid Mechanics*, 12, 481-500.

Hasselmann, K. et al., 1973, Measurements of wind waves growth and swell decay

during the Joint North Sea Wave Project (JONSWAP), *Dt. Hydrogr. Z.*, A8(12), 95p.
Hasselmann, S. and K. Hasselmann, 1981, A symmetrical method of computing the nonlinear transfer in a gravity wave spectrum, *Hamb. Geophys.Einzelschriften, Reihe A:Wiss. Abhand.*, 52, 138p.
Hasselmann, S. and K. Hasselmann, 1985, Computations and Parameterizations of the Nonlinear Energy Transfer in a Gravity-Wave Spectrum. Part I: A New Method for Efficient Computations of the Exact Nonlinear Transfer Integral, *Journal of Physical Oceanography*, 15, 1378-1391.
Komatsu, K., T. Kusaba and A. Masuda, 1993, An efficient method for computing nonlinear energy transfer among wind waves, *Bull. Res. Inst. Appl. Mech. Kyushu Univ.*, 75, 121-146 (in Japanese).
Komatsu, K. and A. Masuda, 1996, A new scheme of nonlinear energy transfer among wind waves: RIAM method – algorithm and performance -, *Journal of Oceanography*, 52, 509-537.
Komatsu, K. 1996, Development of a new generation wave forecasting model based on a new scheme of nonlinear energy transfer among wind waves, *Dr. Thesis, University of Kyushu*, 155p. (in Japanese).
Komatsu, K and A. Masuda, 2000, The RIAM scheme for computing nonlinear energy transfer among wind waves at finite depths, *Reports of the Section of Laboratory Experiment, Dynamics Simulation Research Center, Research Institute for Applied Mechanics, Kyushu University*, No. 3, 119-136 (in Japanese).
Masuda, A, 1980, Nonlinear energy transfer between wind waves, *Journal of Physical Oceanography*, 10, 2082-2092.
The WAMDI Group (13 Authors), 1988, The WAM model -A third generation ocean wave prediction model, *Journal of Physical Oceanography*, 18, 1378-1391.
Tracy, B. A. and D. T. Resio, 1982, Theory and calculation of the nonlinear energy transfer between sea waves in deep water, *U. S. Army Engineer Waterways Experimental Station, Rep. No. 11*, Vicksburg, U. S. A.
Ueno, K. and M. Ishizaka, 1997, On an efficient calvulation method of the nonlinear energy transfer in wind waves, *Sottukojiho*, JMA, 64, 75-80 (in Japanese).
Resio, D. and W. Perrie, 1991, A numerical study of nonlinear energy fluxes due to wave-wave interactions, *Journal of Fluid Mechanics*, 223, 603-629.
Webb, D. J., 1978, Non-linear transfers between sea waves, *Deep-Sea Res.*, 25, 279-298.
Young, I. and L. Verhagen, 1996, The growth of fetch limited waves in water of finite depth. Part 2. Spectral evolution, *Coastal Engineering*, 29, 79-99.

Key words for

FOUR-WAVE INTERACTIONS IN SWAN

by Noriaki Hashimoto, IJ. G. Haagsma, and L. H. Holthuijsen

wave-wave interactions
numerical wave model
shallow water waves
SWAN
numerical techniques
spectral evolution
Lake George